OPTIMIZED LINEAR ACTIVE DISTURBANCE REJECTION CONTROL OF SERVO VALVE-CONTROLLED CYLINDER SYSTEM IN ELECTRO-HYDRAULIC HITCH

/

电液悬挂装置伺服阀控缸系统线性自抗扰优化控制

Yong WANG* [1, 4], Qiwen WANG[1], Xukai WANG[2], Lizhong LU[3], Zhengyi SUN [1, 4]

[1] School of Intelligent Manufacturing and Elevator, Huzhou Vocational and Technical College, Huzhou / China;

[2] School of Engineering, Huzhou University, Huzhou / China;

[3] School of Mechanical Engineering, Zhejiang University of Technology, Hangzhou / China;

[4] Key Laboratory of Robot System Integration and Intelligent Equipment of Huzhou, Huzhou / China;

Tel: +086-15958045607; E-mail: yong_wang@huvtc.edu.cn

DOI: https://doi.org/10.35633/inmateh-78-39

Keywords: *Agricultural tractor electro-hydraulic hitch system, Servo valve-controlled cylinder system, Linear active disturbance rejection control (LADRC), Genetic algorithm (GA), MATLAB-AMESim co-simulation*

ABSTRACT

As the core component of the tractor operation system, the electro-hydraulic hitch system is the key equipment to realize the implement hitching, lifting adjustment, tillage depth control and adaptive posture control. The hydraulic valve-controlled cylinder system serves as the core control unit of agricultural tractor electro-hydraulic hitch systems. Given that the hydraulic system of tractor hitch devices exhibits strong nonlinearity, uncertainty, and time varying parameters, this study focuses on the valve-controlled cylinder electro-hydraulic servo system and proposes a composite control strategy that integrates linear active disturbance rejection control (LADRC) with parameter optimization via genetic algorithm (GA). This strategy utilizes the linear extended state observer (LESO) of LADRC to estimate and compensate for the total disturbance of the system in real time, while adaptively adjusting the parameters of LADRC using the multi objective optimization characteristics of GA, overcoming the problems of observation lag and gain conflict in traditional trial and error parameter tuning. To verify the control performance, a co-simulation model of the servo valve-controlled cylinder system based on MATLAB-AMESim platform was constructed. The simulation results demonstrate that GA-LADRC achieve significantly superior control performance compared to the PID controller, and in step signal tracking, GA-LADRC reduces both the overshoot and tracking error by more than 50% compared to general LADRC. For sinusoidal signal tracking, GA-LADRC exhibits an 18% reduction in phase lag, an 18.3% improvement in accuracy, and a 34.8% decrease in the integral square error (ISE) compared to general LADRC. Furthermore, under disturbance conditions, GA-LADRC also demonstrates superior anti-interference ability. These results confirm the stability and effectiveness of the proposed GA-LADRC strategy, and the developed method is expected to provide technical support for the fine plowing operation of tractors.

摘要

电液悬挂装置作为拖拉机作业系统的核心组成部分，是实现农具挂接、升降调节、耕深控制及作业姿态自适应的关键装备，液压阀控缸系统是农用拖拉机电液悬挂装置的核心控制单元。针对拖拉机悬挂装置液压系统具有强非线性、不确定性和时变参数的特点，本研究以阀控缸电液伺服系统为研究对象，提出了一种融合线性自抗扰控制（LADRC）与遗传算法（GA）参数优化的复合控制策略。该策略通过 LADRC 的扩张状态观测器（LESO）实时估计并补偿系统总扰动，同时利用 GA 的多目标优化特性自适应调节 LADRC 的参数，克服传统试凑法参数整定中存在的观测滞后与增益冲突。为验证控制性能，构建了基于 MATLAB-AMESim 平台的联合仿真模型。仿真结果表明，在阶跃响应和正弦跟踪仿真试验中，GA-LADRC 的控制效果明显优于 PID；且 GA-LADRC 在阶跃信号仿真分析中，相较于传统 LADRC 在超调量和跟踪误差上均降低了 50%以上；在正弦信号跟踪中，GA-LADRC 相较于传统LADRC 相位滞后降低18%，精度提高18.3%，ISE 降低34.8%。此外，在干扰条件下，GA-LADRC 还表现出优越的抗干扰能力。研究结果表明，所提出的 GA-LADRC 方法稳定有效，可为拖拉机精耕作业提供技术支持。

INTRODUCTION

The hydraulic hitch control system is a critical component in large agricultural tractors, serving as the core element for power transmission and intelligent control in high power tractor field operations.

The performance of hydraulic hitch control directly influences tractor operational efficiency and implement energy consumption *(Mattetti et al., 2017; Balsari et al., 2021)*. Primary control methods for agricultural tractor hydraulic hitch systems include position control *(Shekh et al, 2014)*, slip rate control *(Gupta et al., 2019)*, integrated draught position control *(Liu et al., 2023)*, vibration damping control *(Cheng et al., 2017)*, and pressure control *(Liu et al, 2020)*.

Position control represents a common mode for tractor plowing operations, and scholars have conducted extensive research on electro-hydraulic hitch position control during plowing tasks. Soylu et al. proposed an automatic slip control system based on fuzzy logic for agricultural tractors, which automatically adjusts the tillage depth by monitoring the slip during plowing, significantly improving tillage efficiency (*Soylu et al, 2021*). Sabouri et al. Installed an electro-hydraulic depth control system on the tractor and developed an online control algorithm suitable for precision farming, which can adjust the depth of the tiller according to the positioning of hard soil layers (*Sabouri et al, 2021*). Xiao et al. designed a tillage depth regulation system for rotary tillers utilizing fuzzy PID control, demonstrating that this control strategy enables rapid and accurate attainment of target tillage depth *(Xiao et al., 2023)*.

To achieve high performance tracking control of electro-hydraulic servo systems for improved position control, researchers have applied various adaptive algorithms to such systems. Cho et al. adopted a load sensing position tracking control strategy for a valve-controlled cylinder system using a variable displacement pump with constant speed, which significantly reduces the input energy of the pump while maintaining the same position tracking control accuracy (*Cho et al., 2012*). Mihalev et al. conducted research on robust control for electro-hydraulic tracking systems; compared with PI control, the electro-hydraulic system employing robust control demonstrated enhanced operational performance and stability (*Mihalev et al., 2022*). Olranthichachat et al designed an optimal robust PI controller for an electro-hydraulic servo system, utilizing the particle swarm optimization algorithm to simplify the solution process of the structured robust control problem *(Olranthichachat et al., 2011)*. Guo et al. compared the control performance of ADRC and PID on valve-controlled cylinder electro-hydraulic servo systems through MATLAB-AMESim co-simulation, and found that ADRC has strong robustness and high control accuracy in electro-hydraulic servo systems, but requires numerous parameters to be adjusted *(Guo et al., 2020)*. Duan et al. proposed a third-order active disturbance rejection control method based on advance prediction to improve the dynamic performance of servo valve controlled hydraulic motors, and solved the phase lag problem of ADRC by introducing advance prediction *(Duan et al., 2024)*. Hu and Li optimized the LADRC controller of valve-controlled hydraulic motor, replaced the nonlinear function of ESO in the generalized ADRC with arc hyperbolic sine function to reduce jitter *(Hu et al., 2020)*. The ADRC controller does not rely on the precise mathematical model of the system, but considers model uncertainty, nonlinearity, and internal and external disturbances as total disturbances. Compared with PID control systems, it exhibits better dynamic performance and stronger anti interference ability *(Gao et al., 2023; Shi et al., 2018)*. However, the parameter tuning of the ADRC controller in the above research work is mainly based on empirical selection and cannot be adaptively adjusted, which cannot well meet the requirements of high performance electro-hydraulic servo systems.

In order to further improve the control performance of electro-hydraulic servo control system in agricultural tractor hitch, this paper proposes a composite control strategy that combines LADRC and genetic algorithm (GA) for servo valve-controlled cylinder system. In this strategy GA is employed to adaptively adjust the LADRC parameters. Based on the AMESim and MATLAB/Simulink joint simulation platform, the mechanical hydraulic model of servo valve-controlled cylinder system is built, and the actual working condition factors such as nonlinear friction of valve core, leakage of hydraulic cylinder and load disturbance are fully considered for joint simulation analysis. The co-simulation results show that compared with traditional PID and LADRC controllers, the GA-LADRC controller proposed in this paper has better robustness and faster response speed, which has great application scenarios and practical value, and providing reference for the control research of electro-hydraulic servo systems.

MATERIALS AND METHODS

MATHEMATICAL MODEL OF SERVO VALVE-CONTROLLED CYLINDER SYSTEM

Working principle

The servo valve-controlled cylinder system mainly consists of a servo valve body module, servo motor, mechanical transmission part, linear variable displacement transformer (LVDT) sensor, and hydraulic cylinder. The system composition is shown in Figure 1.

When the motor drive controller receives an external signal, the servo motor converts the input current signal into rotor angular displacement. Angular displacement drives the valve core to rotate through a rotating sliding mechanical structure.

The rotation of the valve core is converted into axial displacement by a hydraulic servo screw mechanism, thereby controlling the flow of oil into the hydraulic cylinder. LVDT sensors are installed inside the hydraulic cylinder to receive displacement signals from the hydraulic cylinder piston and form closed loop feedback, thereby achieving displacement control of the hydraulic cylinder piston.

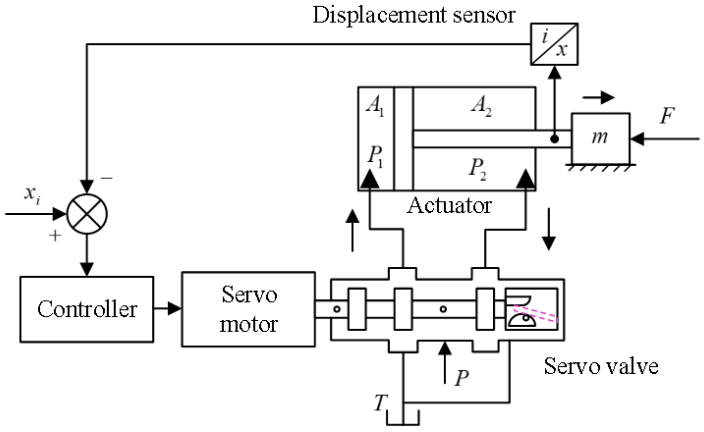

Fig. 1 - Composition of servo valve-controlled cylinder system

Mathematical modeling

- ***Mathematical model of servo valve***

According to the working principle of a servo valve *(Li et al., 2016)*, the flow rate from the high pressure groove into the spiral groove and the flow rate from the spiral groove into the low pressure groove can be expressed as:

$$q_1 = C_d A_1 \sqrt{\frac{2}{\rho}}(P_s - P_c) \tag{1}$$

$$q_2 = C_d A_2 \sqrt{\frac{2}{\rho}} P_c \tag{2}$$

where q_1 is the inflow flow rate of the spiral groove; q_2 is the outflow flow rate of the spiral groove; C_d is the flow coefficient; A_1 is the overlapping area between the high pressure groove and the spiral groove; A_2 is the overlapping area between low pressure groove and spiral groove; ρ is the density of the oil; P_s is the system pressure; P_c is the sensitive chamber pressure.

The overlapping areas of high pressure groove, low pressure groove and spiral groove can be expressed as:

$$A_1 = -R\theta\omega + \frac{2\omega h_0}{\sin\beta} \tag{3}$$

$$A_2 = 2R\theta\omega + \frac{2\omega h_0}{\sin\beta} \tag{4}$$

where R is the piston radius; θ is the rotation angle of the piston; β is the inclination angle of the inclined groove; h_0 is the initial overlap height between the high pressure groove and the inclined groove; ω is the width of high pressure groove.

The specific relationship between the axial movement and circumferential rotation of the servo valve piston can be expressed by combining the expression of the height change Δh of the overlap between the high and low pressure grooves and the inclined groove when considering the rotation and axial movement of the piston:

$$\Delta h = R\theta \sin\beta - x_v \cos\beta \tag{5}$$

From the flow continuity equation, the flow rate within the sensitive chamber can be obtained as follows:

$$q_1 - q_2 = A_s \frac{dx_v}{dt} + \frac{V_c}{\beta_e}\frac{dP_c}{dt} \tag{6}$$

where A_s is the working area of the sensitive cavity; x_v is the axial displacement of the valve core; V_c is the volume of the sensitive cavity; β_e is the bulk modulus of elasticity of the oil.

The motion equation of the valve core can be expressed as:

$$P_c A_s - P_s A_L = m\frac{d^2x_v}{dt^2} + B_s\frac{dx_v}{dt} + K_s x_v + F_L \tag{7}$$

where A_L is the working area of the high pressure chamber; m is the mass of the valve core; B_s is the damping of the valve core; K_s is the spring stiffness; F_L is the load on the valve core.

According to Eqs. 1-7, the system block diagram of servo valve core shown in Figure 2 can be obtained.

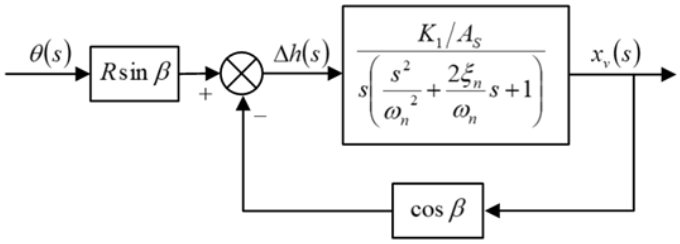

Fig. 2 - Control block diagram of servo valve core

It can be seen that the transfer function of the displacement of the valve core relative to the rotation angle θ of the valve core can be expressed as:

$$\frac{x_v(s)}{\theta(s)} = \frac{R\sin\beta}{\frac{s\left(\frac{s^2}{\omega_n{}^2}+\frac{2\xi_n}{\omega_n}s+1\right)}{K_1/A_S}+\cos\beta} \tag{8}$$

In the equation, ω_n is the natural frequency of the valve piston, K_1 is the flow gain coefficient of the valve piston, and ξ_n is the damping ratio of the valve piston.

$$\omega_n = \sqrt{\frac{{A_s}^2\beta_e}{mV_c}} \quad , \quad \xi_n = \frac{\sqrt{\frac{{A_s}^2\beta_e}{mV_c}}}{2{A_s}^2}\left(\frac{B_P V_c}{\beta_e} + mK_2\right) \quad , \quad K_1 = 2C_d\omega\sqrt{\frac{P_s}{\rho}} \quad , \quad K_1 = 2C_d\omega\sqrt{\frac{P_s}{\rho}}$$

where K_2 is the pressure flow gain coefficient of the valve piston; B_p is the total viscosity coefficient acting on the valve core.

- ***Mathematical model of valve-controlled cylinder***

Assuming that the return oil pressure P_0 is zero and the supply oil pressure P_s is constant, the linearized flow equation of the servo valve can be written as:

$$Q_1 = 2C_d\omega x_v\sqrt{\frac{2}{\rho}}(P_s - P_1) \tag{9}$$

$$Q_2 = 2C_d\omega x_v\sqrt{\frac{2}{\rho}}P_2 \tag{10}$$

where Q_1 and Q_2 are the flow rates of the hydraulic cylinder entering and exiting the oil chamber; C_d is the flow coefficient; P_1 and P_2 are the pressures of the hydraulic cylinder entering and exiting the oil chamber.

In an ideal situation, the continuity equation for hydraulic cylinder flow is:

$$Q_L = A_P\frac{dy}{dt} + \frac{V_t}{4\beta_e}\frac{dP_L}{dt} + C_{ip}P_L \tag{11}$$

In this equation, $Q_L = (Q_1 + Q_2)/2$ is the load flow rate; A_p is the effective area of the piston; y is the displacement of the piston; V_t is the total volume of the hydraulic cylinder; β_e is the equivalent bulk modulus of elasticity of the oil; C_{ip} is the leakage coefficient; P_L is the load pressure.

The force balance equation of the hydraulic cylinder can be expressed as:

$$A_1P_1 - A_2P_2 = A_PP_L = My + By + Ky + F \tag{12}$$

where M is the total mass of the piston and load; B is the viscous damping coefficient; K is the elastic stiffness; F is the external load.

By linearizing the equation, the load flow Q_L is obtained as:

$$Q_L = k_qx_v - k_cP_L \tag{13}$$

In the equation, k_q is the flow gain; k_c is the flow pressure coefficient.

By applying the Laplace transform to Eqs. (11-13), the following set of equations is obtained:

$$\begin{cases} Q_L = k_qx_v - k_cP_L \\ Q_L = C_{ip}P_L + \frac{V_t}{4\beta_e}sy + A_PsP_L \\ A_PP_L = Ms^2y + Bsy + Ky + F \end{cases} \tag{14}$$

The block diagram of valve controlled hydraulic cylinder system drawn from Equation 14 is shown in Figure 3:

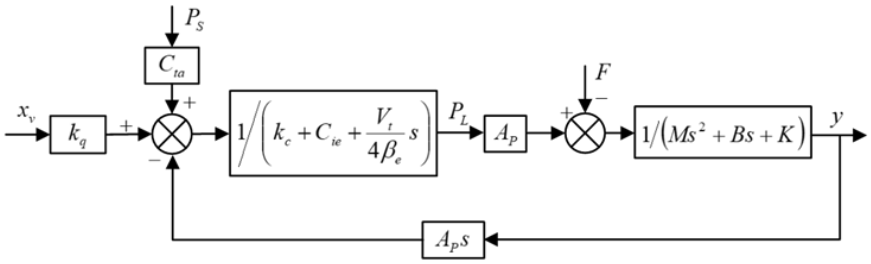

Fig. 3 - Block diagram of valve-controlled hydraulic cylinder system

When the axial displacement x_v of the valve core and the external load force F act simultaneously, the output displacement of the hydraulic cylinder piston can be obtained as:

$$Y(s)=\frac{(k_P/A_P)x_v+Q_{ea}/A_P-[K_{ta}+(V_t/4\beta_e)s]F/{A_P}^2}{\frac{V_t m}{4\beta_e {A_P}^2}s^3+\left(\frac{V_t B}{4\beta_e {A_P}^2}+\frac{K_{ta}m}{{A_P}^2}\right)s^2+\left(\frac{V_t K}{4\beta_e {A_P}^2}+\frac{K_{ta}B}{{A_P}^2}+1\right)s+\frac{K_{ta}K}{{A_P}^2}} \quad (15)$$

In this equation, $K_{ta}=k_c+C_{ie}$ is the total flow pressure coefficient and $Q_{ea}=C_{ia}+P_S$ is the additional leakage flow rate.

In hydraulic cylinder systems, inertia loads are usually the main load, and the viscous friction coefficient B is very small, and the total flow pressure coefficient K_{ta} is also very small. The coupling effect BK_{ta}/A_P will be very small, that is $BK_{ta}/A_P \ll 1$, which can be ignored. Therefore, $Y(s)$ can be simplified as:

$$Y(s)=\frac{(k_P/A_P)x_v+Q_{ea}/A_P-F(s)[K_{ta}(1+V_t s/4\beta_e K_{ta})]/{A_P}^2}{\left[\frac{V_t m}{4\beta_e {A_P}^2}s^2+\left(\frac{V_t B}{4\beta_e {A_P}^2}+\frac{K_{ta}m}{{A_P}^2}\right)s+1\right]s}=\frac{\left((k_P/A_P)x_v+Q_{ea}/A_P-F(s)[K_{ta}(1+V_t s/4\beta_e K_{ta})]/{A_P}^2\right)}{\left(\frac{s^2}{{\omega_h}^2}+\frac{2\xi_h}{\omega_h}s+1\right)s} \quad (16)$$

where ω_h is the hydraulic natural frequency, and ξ_h is the hydraulic damping ratio:

$$\omega_h=\sqrt{\frac{4{A_P}^2\beta_e}{mV_c}}\ ,\ \xi_h=\frac{K_{ta}}{A_P}\sqrt{\frac{\beta_e m}{V_t}}+\frac{B}{4A_P}\sqrt{\frac{V_t}{\beta_e m}}$$

The transfer function of the hydraulic cylinder piston displacement $Y(s)$ relative to the given input valve spool displacement $x_v(s)$ can be expressed as:

$$\frac{Y(s)}{x_v(s)}=\frac{k_q/A_P}{s\left(\frac{s^2}{{\omega_h}^2}+\frac{2\xi_h}{\omega_h}s+1\right)} \quad (17)$$

DESIGN OF VALVE-CONTROLLED CYLINDER CONTROLLER BASED ON GA-LADRC

In order to improve the control performance of the servo valve-controlled cylinder system, this paper proposes a control strategy based on LADRC to achieve precise control of piston rod displacement, GA is used to tune the parameters of LADRC controller to solve the problem of difficulty in adjusting parameters of conventional LADRC controller. The corresponding control system diagram is shown in Figure 4. The controller directly controls the linear movement of the servo valve spool by controlling the deflection angle of the servo motor, changes the flow rate output by the servo valve, and then controls the displacement output of the hydraulic cylinder piston rod. The output displacement is recognized and collected by an embedded LVDT sensor and fed back to the input. In each control period, LADRC controller is optimized and iterated by GA, and the control signal is output again to achieve tracking control of the input displacement.

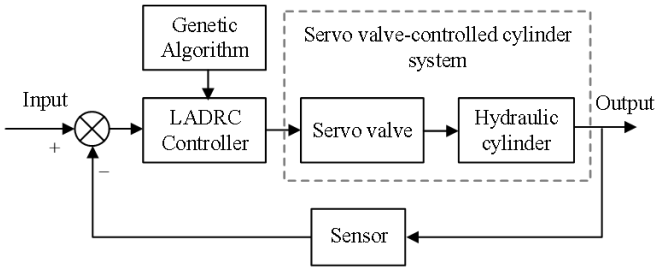

Fig. 4 - Structure diagram of control system

LADRC controllers generally consist of three parts: linear tracking differentiator (LTD), linear extended observer (LESO), and linear state error feedback law (LSEF). The controlled object model has three orders, therefore a third-order LADRC controller is designed. The corresponding control block diagram is shown in Figure 5.

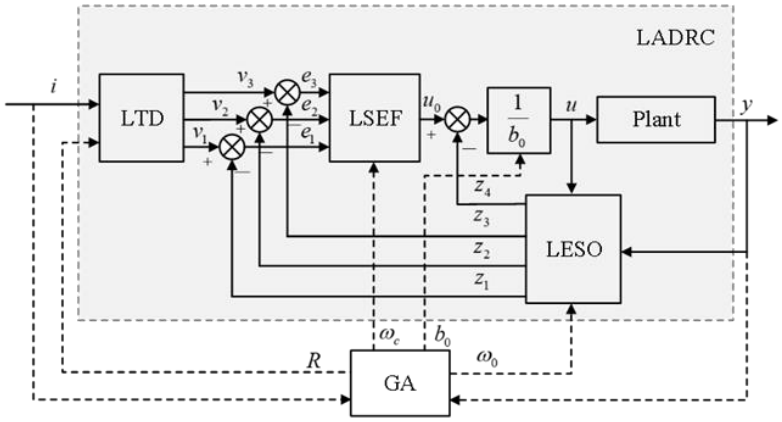

Fig. 5 - Third order GA-LADRC control block diagram

Linear tracking differentiator

LTD is mainly aimed at smoothing the abrupt noise of the reference signal, avoiding input signal oscillation and abrupt changes, while retaining the dynamic characteristics of the signal, helping LESO more accurately estimate the internal and external disturbances of the system, and enhancing anti interference ability. For a third-order electro-hydraulic servo system, it is necessary to track the position, velocity, acceleration, and other characteristics of the hydraulic cylinder to generate smooth transition signals and avoid overshoot. The LTD expression is shown as follows:

$$\begin{cases} \dot{v}_1 = v_2 \\ \dot{v}_2 = v_3 \\ \dot{v}_3 = -R^3(v_1 - v) - 3R^2 v_2 - 3R v_3 \end{cases} \quad (18)$$

where v is the input signal; v_1, v_2, v_3 are the derivatives of the input signal; R is the tracking speed adjustment factor.

Linear extended state observer

The LESO is the key part of the LADRC, which is used to solve the core problem of disturbance observation. By treating the dynamic characteristics, parameter perturbations, and unmodeled features of the system as the total disturbance and extending them as additional state variables, the joint estimation of system state and disturbance is achieved. The fourth-order linear extended state observer obtained by augmenting a third-order system with a total disturbance state, is expressed as:

$$\begin{cases} \dot{z}_1 = z_2 + \beta_1(y - z_1) \\ \dot{z}_2 = z_3 + \beta_2(y - z_1) \\ \dot{z}_3 = z_4 + \beta_3(y - z_1) + b_0 u \\ \dot{z}_4 = \beta_4(y - z_1) \end{cases} \quad (19)$$

where β_1, β_2, β_3 are the observer gains, which can be tuned via the observer bandwidth ω_0.

$$\beta_1 = 4\omega_0, \beta_2 = 6{\omega_0}^2, \beta_3 = 4{\omega_0}^3, \beta_4 = {\omega_0}^4$$

Linear state error feedback law

The LSEF compensates the system disturbance through state error feedback. It is the process of providing error feedback between the system state estimated by the ESO and the reference signal, combined with disturbance compensation to generate the final control input, in order to achieve fast response and precise control. Through LSEF, the displacement of the piston is controlled, and finally the real-time displacement of the piston is fed back to LESO for the next round of control. In this system, LSEF is designed as follows:

$$u_0 = k_p(v_1 - z_1) + k_d(v_2 - z_2) + k_a(v_3 - z_3) \quad (20)$$

where k_p, k_d and k_a are controller gain parameters that can be tuned via the controller bandwidth ω_c

$$k_p = {\omega_c}^3, k_d = 3{\omega_c}^2, k_a = 3\omega_c$$

Removing the total disturbance estimated by the LESO, the final control input obtained after disturbance compensation can be expressed as follows:

$$u = \frac{u_0 - z_4}{b_0} \quad (21)$$

Adaptive parameter adjustment of LADRC by GA

GA is a random search algorithm that simulates the selection, crossover, and mutation of genes during the natural evolution and reproduction process *(Elmouhi et al., 2022; Zhang et al., 2025)*, has been successfully applied to a range of electromechanical design problems, including the optimization of bearingless induction motor control system and permanent magnet couplings *(Yang et al., 2020)*. It has strong global search capabilities and robustness compared to other algorithms. By combining the GA optimization algorithm with the LADRC controller, the optimal parameters that meet the system performance can be found through the iteration of the optimizer, solving the problem of multiple parameters and difficult tuning in high-order LADRC. The algorithm optimization process is shown in Figure 6.

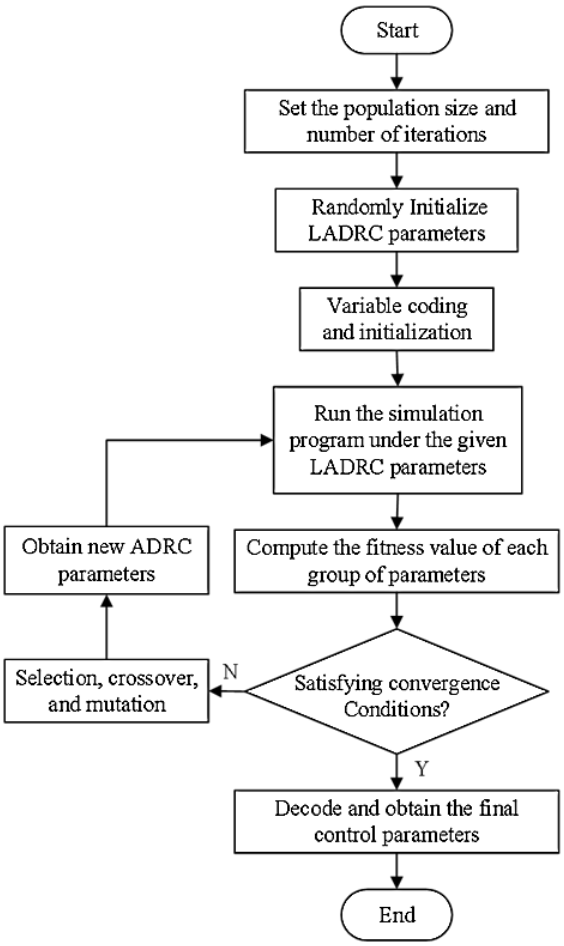

Fig. 6 - Process of parameter tuning of LADRC by GA

In order to achieve better control effects, the steady state error, overshoot, control speed and other performance indicators of the system are considered based on the control requirements of the controlled object. In order to achieve the optimal solution suitable for the current situation, the fitness function is designed as follows:

$$u_0 = k_p(v_1 - z_1) + k_d(v_2 - z_2) + k_a(v_3 - z_3) \quad (22)$$

$ITAE$ is the time absolute error integral, R_a is the smoothness of the controlled system response, σ is the overshoot, a_1, a_2, a_3 are the weights of each indicator. According to the previous analysis, the optimization parameters of LADRC can be as $x = [r, \omega_c, \omega_0, b_0]$.The fitness function is designed as $f(x) = 0.7ITAE + R_a + 0.3\sigma$.

MATLAB-AMESIM COSIMULATION

Model construction of co-simulation

Based on the mathematical model of the servo valve-controlled cylinder, a hydraulic cylinder simulation model is built. At the same time, an external load of 200 N is applied to the piston rod, which is connected to the servo valve to form a complete electro-hydraulic servo system. The output signal of the hydraulic cylinder piston displacement is fed back to the control system built by MATLAB/Simulink to form a complete closed loop. The constructed AMESim model is shown in Figure 7.

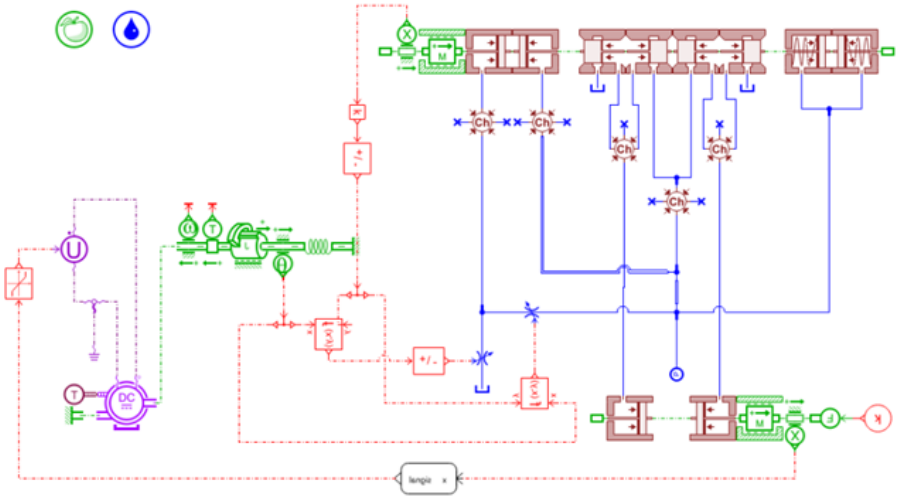

Fig. 7 - AMESim model of electro-hydraulic servo system

The AMESim model established above is used to interact in real time with Simulink software for the hydraulic system simulation model. The designed GA-LADRC co-simulation model is shown as follows:

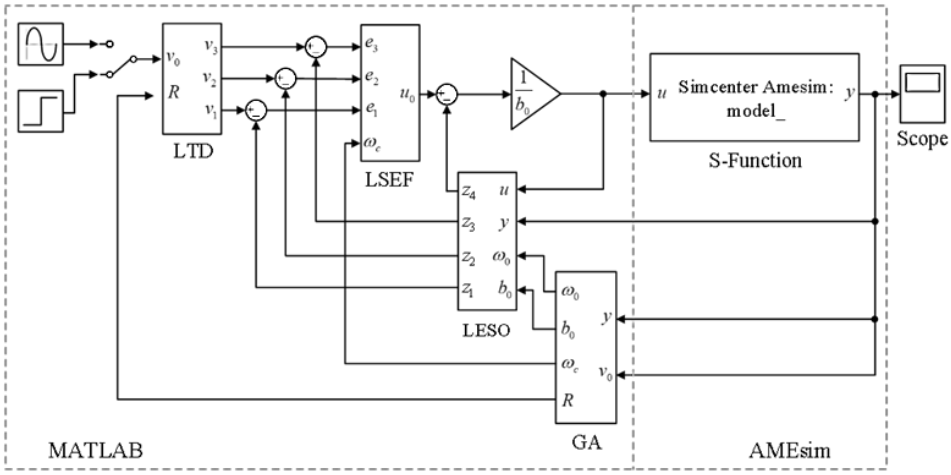

Fig. 8 – Co-simulation model of servo valve-controlled cylinder system based on GA-LADRC

RESULTS

Simulation analysis

Set the initial population of GA as 50 and evolutionary generation as 100. The crossover and mutation probabilities are set as 0.8 and 0.2, respectively, while the elite population is kept at 5%. The final parameters obtained by the GA algorithm are:

$$x = [14.709, 99.976, 116.936, 16413.599]$$

To verify the performance of GA-LADRC control strategy, simulation analysis and comparison with general LADRC and traditional PID controller are carried out. The parameters of GA-LADRC are tuning by genetic algorithm, while the parameters of LADRC and PID are obtained by trial and error method based on response speed, overshoot and smoothness. Parameters of general LADRC controller are set as $R = 12$, $\omega_c = 60$, $\omega_0 = 1500$, $b_0 = 8100$, and traditional PID parameters are set as $k_p = 3.5$, $k_i = 5$.

- ***Simulation analysis of step signal response without disturbance***

In an ideal environment, i.e. without external interference, perform step signal response simulation analysis on the system. When a step signal with a displacement of 80 mm is applied to the system at t=0, the system responses under the action of different controllers are observed. The simulation results are shown in Figure 9 and Table 1.

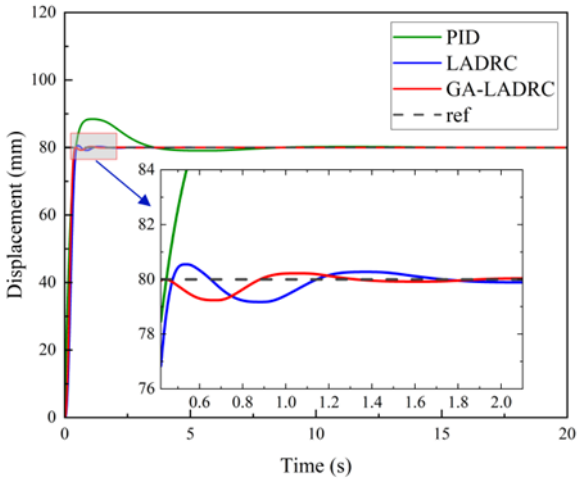

Fig. 9 - Step responses under the action of different controllers without disturbance

Table 1

Control performance under the action of different controllers without disturbance

Controller	Adjustment time	Overshoot	Steady state error e
	[t/s]	[mm]	[mm]
PID	2.93	8.42	0.1763
LADRC	0.48	0.55	0.0013
GA-LADRC	0.44	0.22	0.0006

It can be seen that GA-LADRC has an overshoot of approximately 0.3% in the step response without external interference. Due to the inability of trial and error method to accurately adjust the relationship between various parameters, LADRC has an overshoot of about 0.7% and a slightly longer adjustment time than GA-LADRC. The overshoot of PID is about 10.5% and the adjustment time is 2.93 seconds, which is much larger than LADRC controller.

In the initial response stage, PID control has a faster initial response speed than LADRC due to the effect of the proportional term. However, the PID controller relies on the integral term to accumulate error signals over time, resulting in a convergence time of 6.2 seconds when reaching the input target displacement, which has the worst performance. GA-LADRC and general LADRC use LESO to estimate the system state in real time, combined with LSEF to generate accurate control variables, which can effectively reduce overshoot and oscillation. The system using GA-LADRC controller reaches steady state in 2 seconds, which is better than LADRC and PID control obtained by trial and error method, and has good overshoot and oscillation suppression ability.

- ***Simulation analysis of sinusoidal signal tracking without disturbance***

In order to observe and compare the tracking performance of different controllers for varying displacement, the sinusoidal signal tracking analysis is conducted on the system, and the input displacement sinusoidal signal is set as y=sin(2/5πt), the simulation results are shown in Figure 10 and Table 2.

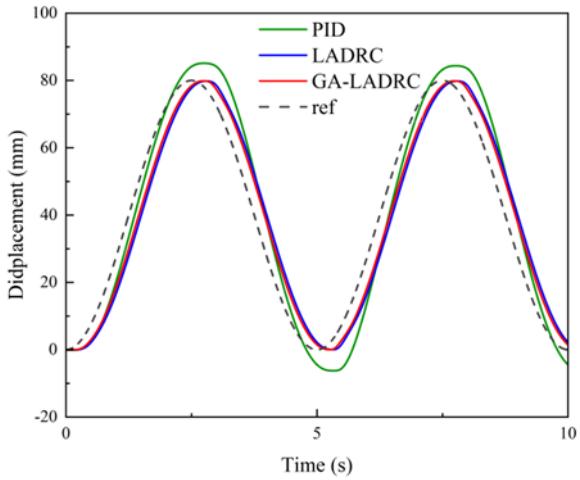

Fig. 10 - Sinusoidal signal tracking effect without disturbance

The control effects of different controllers on disturbance free sinusoidal response can be visually observed, including phase lag, maximum error, and the integral square error (ISE). It can be seen that the PID controller has the maximum error and ISE, but the phase lag is 0.324 rad, slightly better than the LADRC controller. Compared with PID controller, GA-LADRC controller reduces phase lag by 3.1%, improves accuracy by 30%, and reduces ISE by 40.7%. And compared with LADRC, the phase lag is reduced by 18%, the accuracy is improved by 18.3%, and the ISE is reduced by 34.8%. It can be seen that the GA-LADRC controller has better sinusoidal signal tracking and higher accuracy.

Table 2

Sinusoidal tracking performance without disturbance

Controller	Phase lag	Maximum error	ISE
	[t/s]	[mm]	[mm]
PID	0.324	14.73	0.00253
LADRC	0.383	12.46	0.00230
GA-LADRC	0.314	10.18	0.00150

According to Figure 10 and Table 3, the control effects of different controllers on disturbance free sinusoidal response can be visually observed, including phase lag, maximum error, and the integral square error (ISE). It can be seen that the PID controller has the maximum error and ISE, but the phase lag is 0.324 rad, slightly better than the LADRC controller. Compared with PID controller, GA-LADRC controller reduces phase lag by 3.1%, improves accuracy by 30%, and reduces ISE by 40.7%. And compared with LADRC, the phase lag is reduced by 18%, the accuracy is improved by 18.3%, and the ISE is reduced by 34.8%. It can be seen that the GA-LADRC controller has better sinusoidal signal tracking and higher accuracy.

- ***Position control under step disturbance***

To verify the anti-interference performance of the LADRC controller, a step disturbance signal with a displacement of 20 mm was added at the 15th second of the simulation process. From Figure 11 and the enlarged partial view, it can be seen that there are significant differences in the disturbance suppression ability of different controllers after the electro-hydraulic servo system is subjected to step disturbances. Among them, GA-LADRC outperforms LADRC and PID controllers in terms of maximum deviation, regulation time, and steady state error. The maximum deviation of the PID controller after interference is 2.98 mm, and the maximum deviation and interference adjustment time are about 5 times and 2 times that of LADRC, which confirms that LADRC has stronger anti interference ability than the PID controller. At the same time, the anti-interference ability of GA-LADRC has been improved on the basis of LADRC. Based on the above factors, GA-LADRC has the best control effect and performance.

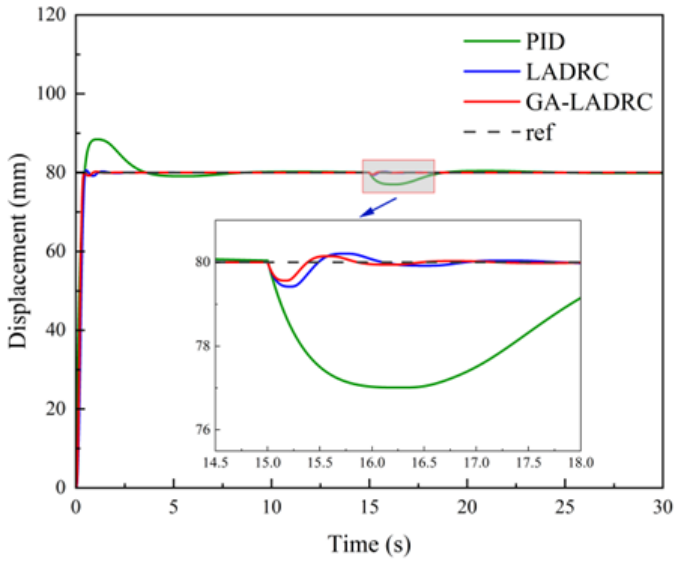

Fig. 11 - Simulation results of displacement control considering disturbance

Table 3

Performance of step disturbance control

Controller	Maximum offset x	Adjustment time	Steady state error e
	[mm]	[t/s]	[mm]
PID	2.98	3.84	0.1400
LADRC	0.58	1.92	0.0030
GA-LADRC	0.45	1.20	0.0014

- ***Position control under random disturbance***

In order to further simulate complex situations in actual environments, simulation experiments were conducted by adding random interference signals. Figure 12 shows the random interference signal, which causes the electro-hydraulic servo system to be continuously affected by random external disturbances during displacement control.

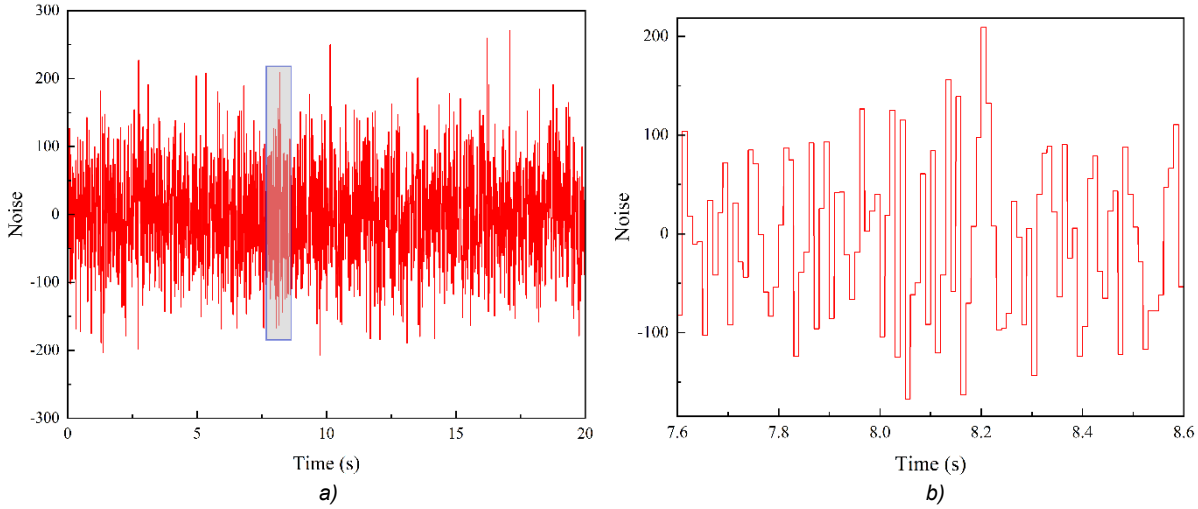

Fig. 12 - (a) Random interference signal; (b) Local zoomed-in view of the random interference signal

Figure 13 shows the simulation results of the system under random interference signals, and at the same time, a segment of the curve is randomly selected for amplification and observation. It can be seen from the figure that the GA-LADRC controller has the least impact compared to the other two controllers. From the enlarged cross section, it can be seen that PID has the largest fluctuation amplitude, while GA-LADRC has the smallest fluctuation amplitude, indicating that GA-LADRC has the best anti interference performance.

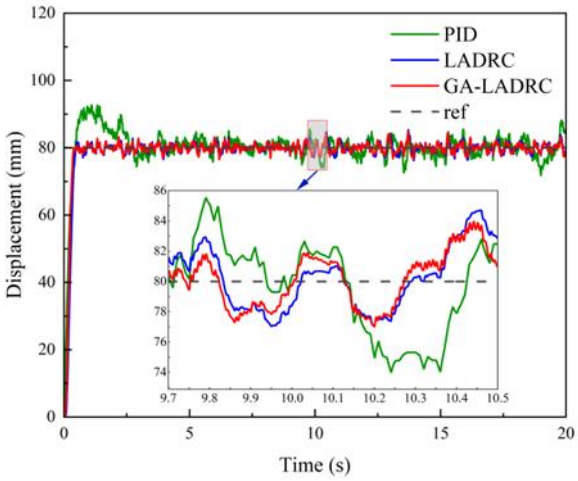

Fig. 13 - Simulation results of position control considering random interference

CONCLUSIONS

This article mainly focuses on improving the performance of the servo valve-controlled cylinder system for agricultural tractor electro-hydraulic hitch, addressing the limitations of traditional PID in position control accuracy and robustness in highly nonlinear servo valve-controlled cylinder systems.

LADRC technology is used to design a controller to overcome the uncertainty and external disturbances of the electro-hydraulic servo system model. Combining GA to automatically adjusting parameters of LADRC to overcome the difficulty of traditional LADRC relying on empirical tuning, shortens the adjustment time, improves the control accuracy of the system, and enhances the anti-interference ability of the valve-controlled cylinder system.

The proposed GA-LADRC strategy demonstrates superior control precision and robustness over both the general LADRC and traditional PID controllers, as evidenced by comparative simulations conducted on the MATLAB-AMESim co-simulation platform. It achieves better performance in both step and sinusoidal tracking scenarios. Upon the introduction of an abrupt disturbance, GA-LADRC restricts the tracking error to 0.45 mm, markedly reducing it compared to the 2.98 mm (PID) and 0.58 mm (LADRC). This leads to more precise positioning and a substantially faster response, effectively elevating the overall system performance of the electro-hydraulic servo control system.

ACKNOWLEDGEMENT

This research was funded by Zhejiang Provincial Basic Public Welfare Research Program of China, grant number (LTGY23E050003) and Huzhou public welfare application research project, grant number (2022GZ49).

REFERENCES

[1] Balsari P., Biglia A., Comba L., Sacco D., Eloi Alcatrão L., Varani M., Mattetti M., Barge P., Tortia C., Manzone M., Gay P., Ricauda Aimonino D., (2021). Performance analysis of a tractor power harrow system under different working conditions. *Biosystems Engineering*, 202, 28-41.

[2] Cheng J., Chi R., Lai Q., Yang Y., Mao E., (2017). Active vibration control of tractor based on electrohydraulic hitch system (基于电液悬挂系统的拖拉机主动减振控制). *Transactions of the Chinese Society of Agricultural Engineering*, 33(5), 82-90.

[3] Cho S. H., Noskievi P., (2012). Position tracking control with load-sensing for energy-saving valve-controlled cylinder system. *Journal of Mechanical Science and Technology*, 26(2):617-625.

[4] Duan Z., Sun C., Li J. T. Y., (2024). Research on servo valve-controlled hydraulic motor system based on active disturbance rejection control. *Measurement and Control: Journal of the Institute of Measurement and Control*, 57(2): 113-123.

[5] Elmouhi N., Essadki A., Elaimani H., (2022). Improved control for DFIG based wind power system under voltage dips using ADRC optimized by genetic algorithms. *International journal of electrical and computer engineering systems*, Jul 15;13(5): 357-67.

[6] Gupta C., Tewari V. K., Ashok Kumar A., Shrivastava P., (2019). Automatic tractor slip draft embedded control system. *Computers and Electronics in Agriculture*, 165, 104947.

[7] Guo W., Zhao Y., Li R., Ding H., Zhang J., (2020). Active Disturbance Rejection Control of Valve-Controlled Cylinder Servo Systems Based on MATLAB-AMESim Cosimulation. *Complexity*, 2020(1): 9163675.

[8] Gao B., Zhang W., Zheng L., Zhao H., (2023). Research on control of electro-hydraulic servo system based on third-order linear ADRC. *Robotic intelligence and automation*; 43(3): 301-12.

[9] Hu Y., Li D., (2020). An improved active disturbance rejection controller for hydraulic valve-controlled hydraulic motor. *In 2020 39th Chinese Control Conference (CCC)*, pp. 6037-6042. IEEE.

[10] Liu C., Jinheng G. U., Xin D. U., Liu C., Yuefeng D. U., Mao E., (2023). Differential and integral sliding mode adaptive control algorithm for draft and position integrated control of electro-hydraulic hitch in agricultural tractor. *INMATEH - Agricultural Engineering*, 70(2).

[11] Liu C., Zhao J., Gu J., Du Y., Mao E., (2020). Pressure Control Algorithm Based on Adaptive Fuzzy PID with Compensation Correction for the Tractor Electronic Hydraulic Hitch. *Applied Sciences*, 10(9), 3179.

[12] Li S., Ruan J., Meng B., (2016). electro-hydraulic proportional directional valve. *Journal of Mechanical Engineering*, 52(2):202-212.

[13] Mattetti M., Varani M., Molari G., Morelli F., (2017). Influence of the speed on soil pressure over a plough. *Biosystems engineering*. 156:136-147.

[14] Mihalev G., Yordanov S., Ormandzhiev K., Kostov K., Mitev, V., (2022). Robust Control of Electro-Hydraulic Servo System. *2022 International Conference Automatics and Informatics (ICAI)*, 2022:218-222.

[15] Olranthichachat P., Kaitwanidvilai S., (2011). Design of Optimal Robust PI Controller for Electro-Hydraulic Servo System. *Engineering Letters*, 19(3):197-203.
[16] Shekh M. I. , Raheman H., Shirvaikar R., Kumar A., (2014). An electromechanical implement lift system with position control for low horse power tractor. *Agricultural Engineering International: CIGR Journal*, 16(4):112-121.
[17] Soylu S., Arman K., (2021). Fuzzy logic based automatic slip control system for agricultural tractors. *Journal of Terramechanics*, 95(7):25-32.
[18] Sabouri Y., Abbaspour Gilandeh Y., Solhjou A., Shaker M., (2021). Development and Laboratory Evaluation of an Online Controlling Algorithm for Precision Tillage. *Sensors*, 21(16):5603.
[19] Shi M., Wang S., Liu H., Wang J., (2018). Research on Electro-hydraulic Servo Passive force control based on ADRC. *In 2018 37th Chinese Control Conference (CCC)*, Jul 25 (pp. 625-630). IEEE.
[20] Xiao M., Ma Y., Wang C., Chen J., Zhu Y., Bartos P., Geng G., (2023). Design and experiment of fuzzy-PID based tillage depth control system for a self-propelled electric tiller. *International Journal of Agricultural and Biological Engineering*. Jul 31;16(4):116-25.
[21] Yang Z., Lu C., Sun X., Ji J., Ding Q., (2020). Study on active disturbance rejection control of a bearingless induction motor based on an improved particle swarm optimization genetic algorithm. *IEEE Transactions on Transportation Electrification*, Oct 15;7(2): 694-705.
[22] Zhang J., Liang Q., Sun J., Yan B., Hu Z., Sun W., (2025). Multi-Objective Optimization of Torque Motor Structural Parameters in Direct-Drive Valves Based on Genetic Algorithm. *Actuators*, 14(11).